

Fatigue-Creep Life Prediction of 2·1/4Cr-1Mo Steel under Combined Tension-Torsion at 600°C

Tatsuo INOUE

Kyoto University, Kyoto, Japan

Shigeru KISHI

Toshiba Corporation, Yokohama, Japan

Hiroyuki KOTO

Mitsubishi Heavy Industries, Ltd., Takasago, Japan

Yukio TAKAHASHI

Central Research Institute of Electric Power Industry, Tokyo, Japan

1 INTRODUCTION

Development of appropriate life prediction methods in the fatigue-creep regime is strongly needed for the design purpose of high temperature machine components exposed to severe operating condition. This paper deals with the second task A-II of the co-operative project (Phase III) and presents the fatigue-creep life prediction under multiaxial stress condition of combined tension-compression and cyclic torsion which is expected to extend the conclusions obtained in Phase-II of the project, being carried out by the Subcommittee on Inelastic Analysis and Life Prediction of High Temperature Materials, JSMS (Members of the Subcommittee are listed in the footnote of the report A-I). Three types of fatigue-creep tests were performed including pure torsion, in-phase and out-of-phase strain-controlled wave patterns, and seven types of life prediction methods were evaluated by comparing the experimental data with the analysis.

2 FATIGUE-CREEP TESTS - PROCEDURE AND RESULTS

2.1 Test conditions

A normalized and tempered 2·1/4Cr-1Mo steel is employed, and ten kinds of fatigue-creep benchmark tests illustrated in Table 1 were performed at 600°C. Fatigue-creep tests for problem II-2(a), II-2(b), III-2(a) and III-2(b) were carried out in Phase II of the project and discussions on the life prediction methods have been conducted [1]. In this paper, we intend to evaluate all of the benchmark test results including other six test results obtained in Phase III.

Thin-walled tubular specimens with outer and inner diameters of 22 mm and 18 mm respectively were used in pure torsion tests, while outer and inner diameters of the specimen in in-phase and out-of-phase tests were 13 mm and 10 mm respectively. This paper also utilizes many kinds of uniaxial data of the identical material acquired in Phase I of the collaborated benchmark project [2, 3].

2.2 Test results

Both uniaxial and multiaxial fatigue-creep lives in experiments are summarized in Fig. 1, where the ordinate expresses the Mises equivalent SMiRT 11 Transactions Vol. L (August 1991) Tokyo, Japan, © 1991

Table 1 Illustration of benchmark problems

Problem (Strain Rate)		Diagram	Problem (Strain Rate)		Diagram
Pure torsion	I (a) ($\dot{\epsilon} = 0.5$ %/s)		Axial-torsion (Out-of-phase)	III-1 (a) ($\dot{\epsilon} = 0.5$ %/s)	
	I (b) ($\dot{\epsilon} = 0.01$ %/s)			III-1 (b) ($\dot{\epsilon} = 0.01$ %/s)	
Axial-torsion (In-phase)	II-1 (a) ($\dot{\epsilon} = 0.5$ %/s)		* The Mises equivalent strain range was taken as 0.8% for all cases.	III-2 (a) ($\dot{\epsilon} = 0.5$ %/s)	
	II-1 (b) ($\dot{\epsilon} = 0.01$ %/s)			III-2 (b) ($\dot{\epsilon} = 0.01$ %/s)	
	II-2 (a) ($\dot{\epsilon} = 0.5$ %/s)				
	II-2 (b) ($\dot{\epsilon} = 0.01$ %/s)				

strain range recommended in the ASME B. & P.V. Code Case N-47. The fatigue lives are notably shorter than the corresponding uniaxial ones in the one of out-of-phase patterns -III-2(a) and III-2(b), while little difference is found between lives in uniaxial and multiaxial stress state in other cases.

3 SUMMARY OF FATIGUE-CREEP LIFE PREDICTION METHODS

Following seven types of fatigue-creep life prediction methods are adopted to evaluate the failure life in this project: They are linear damage rule, strain range partitioning method and methods proposed by Majumdar, Ostergren, Lemaitre-Plumtree-Chaboche and Bui-Quoc, and the Γ -plane method. Since the application to multiaxial stress condition is not clearly stated in some methods in the original papers, some modifications are given to the methods without disturbing the essential concept. The prediction methods employed are briefly reviewed as follows.

(1) Linear Damage Rule (LDR, for brevity)

Following six different ways termed as LDR-1 - 6 are applied in this project, by making some modifications in evaluating fatigue damage D_f and creep damage D_c .

LDR-1: The Mises equivalent strain range and the Mises equivalent stress are adopted to evaluate D_f and D_c respectively as described in the Code Case N-47.

LDR-2: D_f is calculated by the same procedure as LDR-1, and the evaluation of D_c is modified by employing the Huddleston's equivalent stress [4].

LDR-3: D_f is defined as the ratio of experimental life in slow-slow cycling to that in fast-fast pattern under each loading phase condition, and D_c is identified by the same procedure as LDR-1.

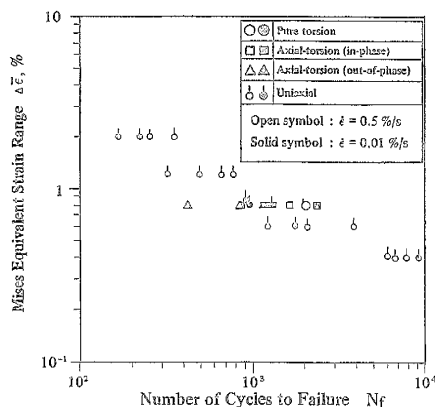


Fig. 1 Summary of experimental results

LDR-4: The same procedure as LDR-3 is applied to calculate D_f , while that of LDR-2 is used for the D_c .

LDR-5: The equivalent strain range along strain path $\Delta \bar{\epsilon}_{\text{path}}$ is defined as

$$\Delta \bar{\epsilon}_{\text{path}} = \frac{1}{2} \int_{\text{cycle}} d\bar{\epsilon} = \frac{1}{2} \int_{\text{cycle}} (d\epsilon^2 + d\gamma^2/3)^{1/2} \quad (1)$$

and the fatigue damage D_f is identified by this value. The same procedure of LDR-1 is also applied in calculating D_c .

LDR-6: D_f and D_c are evaluated by the same procedures as LDR-5 and LDR-2 respectively.

(2) Strain range partitioning method (SRP, for brevity)

The inelastic strain range $\Delta \epsilon_{\text{in}}$ is assumed to be composed of four specific strain components $\Delta \epsilon_{ij}$ under the combination of fast and slow strain waves, and these components are related to the inherent material lives which are represented by the Manson-Coffin type equations:

$$\Delta \epsilon_{ij} \cdot N_{ij}^{\alpha_{ij}} = C_{ij} \quad (2)$$

Fatigue-Creep life can be now estimated by the "Interaction Damage Rule" [5]:

$$1/N_f = \sum (F_{ij}/N_{ij}), \quad F_{ij} = \Delta \epsilon_{ij}/\Delta \epsilon_{\text{in}} \quad (3)$$

The inelastic strain range is partitioned based on the Mises equivalent stress-strain hysteresis loop with the signs of principal stress and strain.

(3) Majumdar method

The crack controlled failure life is given by

$$N_f = [-1 + \{1 + (2D_c/D_t)\}^{1/2}] / D_c \quad (4)$$

with

$$D_c = \int_{\text{cycle}} G_o \epsilon_{\text{eff}}^m \dot{\epsilon}_{\text{eff}}^{k_c} dt, \quad D_t = \int_{\text{cycle}} C_o \epsilon_{\text{eff}}^m \dot{\epsilon}_{\text{eff}}^k dt \quad (5)$$

where ϵ_{eff} is the inelastic shear strain on the maximum inelastic shear strain range plane. The characteristics of failure under multiaxial stress condition is taken into consideration in the material constants, C_o , G_o , k , k_c and m which are the functions of the parameters of η , η' and ξ representing the degree of stress multiaxiality [6].

(4) Ostergren method

Ostergren emphasized the effect of tensile peak stress σ_t during strain cycling as well as a cycle frequency ν on fatigue life, and proposed the equation [7]

$$\sigma_t \Delta \epsilon_{\text{in}} N_f^{\beta} \nu^{\beta(k-1)} = C \quad (6)$$

where β , k and C are the material constants. In applying this method to this project, σ_t and $\Delta \epsilon_{\text{in}}$ are represented by the Mises equivalent stress and inelastic strain ranges respectively.

(5) Lemaitre-Plumtree-Chaboche method

Damage rate equations for D_f of transgranular type cracking and D_c of intergranular type are characterized as [8]

$$dD_f/dN = \{(\sigma_M - \sigma_o)/B(1-D_f)\}^{\beta} (1-D_f)^{-P} \quad (7)$$

$$dD_c/dt = \{|\sigma|/A(1-D_c)\}^x (1-D_c)^{-Q} \quad (8)$$

and the failure is assumed to occur when the sum of D_f and D_c reaches

unity. The Mises equivalent stress-strain hysteresis loop is employed in applying this method.

(6) Bui-Quoc method

The axial fatigue damage D_{fa} and the torsional fatigue damage D_{ft} is assumed to be the function of cycle fraction $\beta_{fa} = n/N_{fa}$ and $\beta_{ft} = n/N_{ft}$ expressed in the form [9]

$$D_{fa} = \beta_{fa} / [\beta_{fa} + (1 - \beta_{fa}) \{r_a - (r_a/r_{au})^8\} / (r_a - 1)] \quad (9)$$

$$D_{ft} = \beta_{ft} / [\beta_{ft} + (1 - \beta_{ft}) \{r_t - (r_t/r_{tu})^8\} / (r_t - 1)] \quad (10)$$

The effects of strain rate $\dot{\epsilon}_f$ and $\dot{\epsilon}_s$ are considered by the equation

$$(N_f)_s / (N_f)_f = (\dot{\epsilon}_s / \dot{\epsilon}_f)^c \quad (11)$$

On applying this method to the multiaxial stress state, the increment of a single representative damage is assumed to be the larger of D_{fa} and D_{ft} in each cycle of the in-phase cycling, while both D_{fa} and D_{ft} are added to the damage in each cycle of the out-of-phase cycling.

(7) Γ -plane method

Brown and Miller [10] have proposed to use the Γ -plane composed of the maximum shear strain range $\Delta\gamma_{max}$ and the normal strain range $\Delta\epsilon_n$ on the plane of maximum shear strain range. In this project, the equivalent shear strain range $\Delta\bar{\gamma}$ is defined based on the test results of Type 304 stainless steel at 550°C and 600°C [11]:

$$\Delta\bar{\gamma} = \frac{1}{1.05} \left(\frac{\Delta\gamma_{max}}{2} + 1.2 \Delta\epsilon_n \right) \quad (12)$$

The fatigue life N_f can be obtained from the characteristics for uniaxial tests using the equivalent shear strain range.

4 RESULTS OF LIFE PREDICTION AND DISCUSSION

4.1 Life Prediction based on experimental stress-strain behavior

The predicted fatigue-creep lives by typical nine prediction methods, in which stress-strain behavior was obtained from the experiment, are summarized in Fig. 2. The life prediction under out-of-phase cycling was executed by LDR, Majumdar method, Bui-Quoc method and Γ -plane method, and following characteristics can be pointed out about the predicted results under out-of-phase wave pattern.

The effect of the definition of equivalent stress on the predicted lives is fairly notable as seen in the comparison of LDR-1 and LDR-2. It follows that the prediction method in term of the Mises equivalent stress overestimates the creep damage, while the Huddleston's stress gives better prediction.

The second remark is that the definition of strain range has little effect on prediction in LDR by the comparison of LDR-2 and LDR-4.

Finally, more preferable predictions can be achieved by the methods by Majumdar and Bui-Quoc than by LDR, since material parameters identified from multiaxial experiments are employed in former methods. The Γ -plane method has almost same accuracy as LDR-2 and LDR-4, when using multiaxial test data of Type 304 stainless steel.

Relating to pure torsion and in-phase cycling, SRP, Ostergren method and Lemaitre-Plumtree-Chaboche method estimate more or less the greater damage than the methods by Majumdar and Bui-Quoc. It may suggest that the Mises

○	Pure torsion	Open symbol : $\dot{\epsilon} = 0.5\%/s$ Solid symbol : $\dot{\epsilon} = 0.01\%/s$
□	Axial-torsion (in-phase)	
△	Axial-torsion (out-of-phase)	

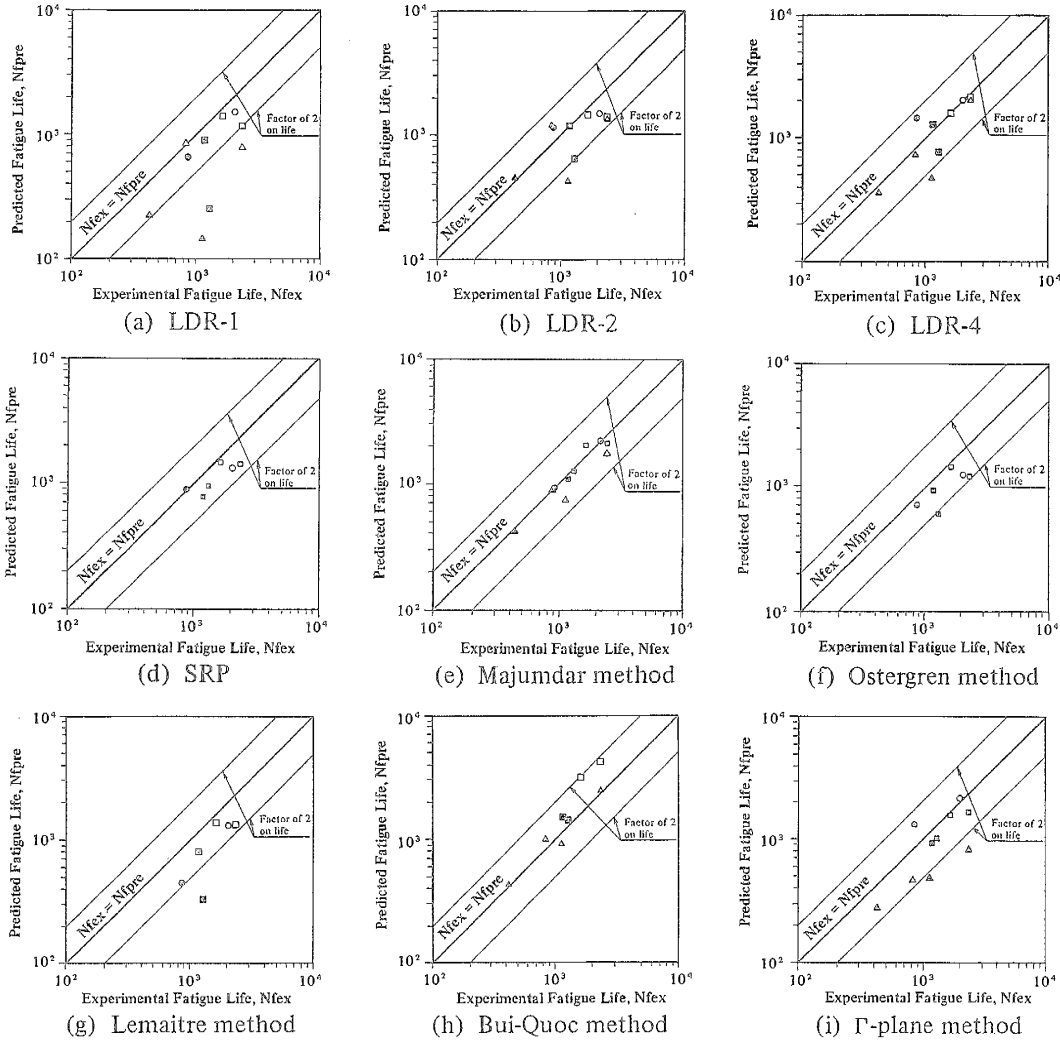


Fig. 2 Comparison of predicted failure life N_{fpre} by different methods with experimental life N_{fex}

equivalent strain is not appropriate for the prediction of multiaxial fatigue-creep lives.

4.2 Life prediction based on the simulated stress-strain relation

The fatigue-creep lives were predicted based on the simulated stress-strain relation in combination with three life prediction methods; LDR, SRP and Majumdar method. Several kinds of inelastic constitutive models, detailed description of which is made in the report of the project A-I, are employed for the evaluation of stress-strain response.

Figure 3 shows that, whatever constitutive models are used, the trends of each prediction method are similar to the corresponding results based on experiments.

5 CONCLUDING REMARKS

From the above discussion on the comparison between predicted and experimental lives in this project, the followings are suggested. The Mises equivalent stress is not a successful parameter to describe the multiaxial fatigue-creep damage, while the Huddleston's stress gives better prediction. SRP, Ostergren method and Lemaitre-Plumtree-Chaboche method give comparatively good estimation of life, though these methods predict more or

less the greater damage than the experiment under pure torsion and in-phase cycling, and cannot predict the life under out-of-phase cycling. The reason is considered to be owing to employment of the Mises equivalent strain, which might be possibly improved by using more sophisticated equivalent strain such as the strain defined on the Γ -plane.

The life prediction based on the analytical stress-strain relation gives almost similar results as that based on the experimental data. It suggests the applicability of the inelastic constitutive models to give the fundamental data for life prediction.

The subcommittee wishes to express her gratitude to the head Committee on High Temperature Strength, JSMS, for supporting the project, and acknowledgement is due to the Ministry of Education and Culture for providing Grant-in-Aid for Co-operative Research A (No. 61302036 and 01302026).

REFERENCES

- [1] Inoue, T., Igari, T., Okazaki, M., Sakane, M. and Tokimasa, K. (1989). Nucl. Engrg. Des., Vol. 114, pp. 311-321.
- [2] Inoue, T., Okazaki, M., Igari, T., Sakane, M. and Kishi, S. (1991). Nucl. Engrg. Des., in print.
- [3] Inoue, T., Ohno, N., Suzuki, A. and Igari, T. (1989). Nucl. Engrg. Des., Vol. 114, pp. 295-309.
- [4] Huddleston, R.L. (1985). J. Press. Vessel. Technol., Vol. 107, pp. 421-429.
- [5] Manson, S.S. and Halford, G.R. (1976). Proc. ASME-MPC Symposium on Creep-Fatigue Interaction, MPC-3, pp. 299-322.
- [6] Majumdar, S. (1981). Nucl. Engrg. Des., Vol. 63, pp. 121-135.
- [7] Ostergren, W.J. (1976). J. Testing and Evaluation, Vol. 4, pp. 327-339.
- [8] Lemaitre, J. and Plumtree, A. (1979). Trans. ASME, J. Engrg. Mater. Technol., Vol. 101, pp. 284-292.
- [9] Gomuc, R., Bui-Quoc, T. and Biron, A. (1987). Res. Mechanica, Vol. 21, pp. 135-154.
- [10] Brown, M.W. and Miller, K.J. (1982). ASTM STP770, pp. 482-499.
- [11] Ogata, T., Nitta, A. and Kuwabara, K. (1988). Central Research Institute of Electric Power Industry Report, T87058.

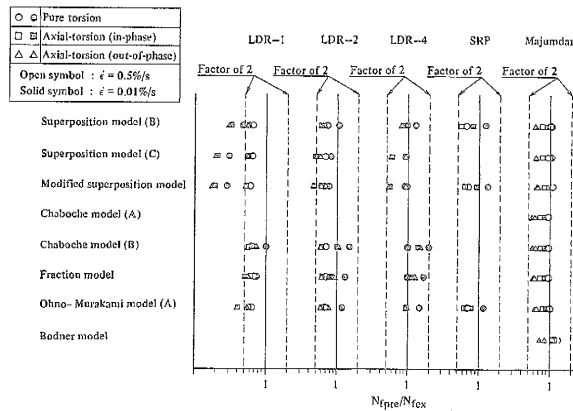


Fig. 3 Predicted results combining several kinds of constitutive models